64455

Oriented, Glass-coated Impact Melt Rock

56.7 grams

Figure 1: Original PET photo of dusty glass egg 64455 in its upside down position (resting on zap pits). Scale is in cm. NASA # S72-40132. (compare with figure 11)

Introduction

Sample 64455 has proven to be a nearly perfect sample for studies of the effects of comic ray, solar comic ray and micrometeorite bombardment of the lunar surface over the last 2 My, because it apparently maintained its orientation since it landed and been continuously exposed to the space environment for that time.

64455 is an egg-shaped object about 5 cm long and 3 cm across (figure 1) almost completely covered with thick black glass. The inside "yoke" is a fragment of basaltic melt rock, which is exposed in one quadrant on the top where the glass has broken off. The top surface is almost completely covered with micrometeorite craters, while the bottom surface has none, indicating that the sample has maintained its orientation since it landed on the lunar surface (figure 2).

Petrography

Sample 64455 is a basaltic impact melt with very thick glass coat (Ryder and Norman 1980). Grieve and Plant (1973) describe four texture zones (a) interior fractured highland basalt, (b) basalt with interstitial partial melt, (c) a thin crust of brown devitrified glass, and (d) an outer coating of fresh glass (figure 3). Vaniman and Papike (1980) group the crystalline highland basalt interior fragment with the Low-K Fra Mauro suite and give the mineralogical mode as 59.9 vol. % plagioclase, 32.7 % pyroxene, 6.5 % olivine (with trace metal, troilite, schreibersite and "rust").

Mineralogy

The composition of pyroxene, olivine and plagioclase of the interior rock fragment are presented in Vaniman and Papike (1980) and Heiken et al. (1991) (figures 4 and 5). The composition of schreibersite and metal

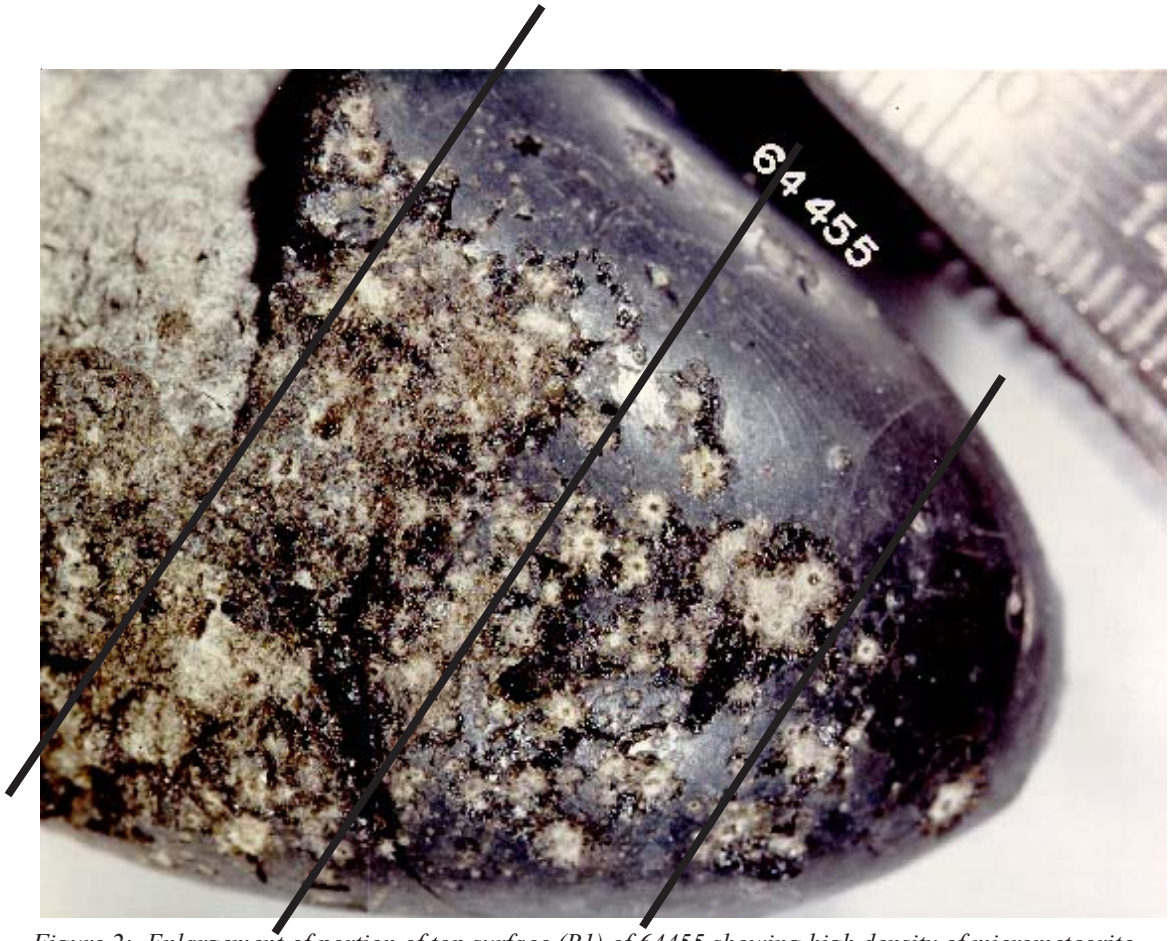

Figure 2: Enlargement of portion of top surface (B1) of 64455 showing high density of micrometeorite "zap" pits and approximate position of saw cuts. Photo # S73-22656. Scale in mm is shown.

Figure 3: Photomicrograph of thin section of interior basalt fragment in 64455 (from Grieve and Plant 1973).

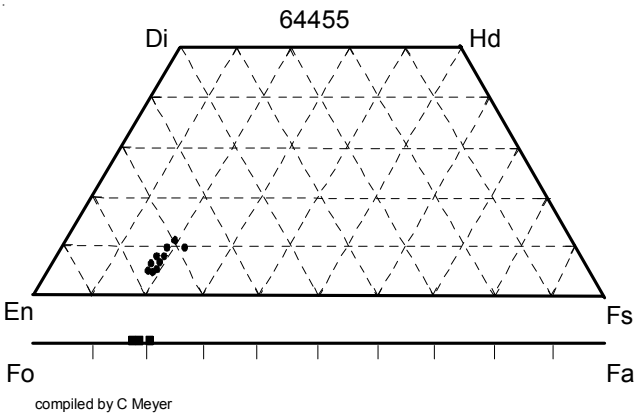

Figure 4: Pyroxene and olivine composition of interior "highland basalt" rock inclusion in 64455. Data replotted from Vaniman and Papike (1980) with appologies.

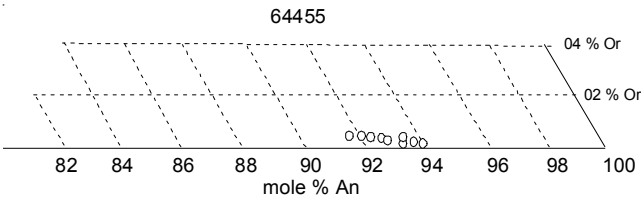

Figure 5: Plagioclase composition in basalt fragment in 64455 (from Vaniman and Papike, 1980).

grains are given in Grieve and Plant (1973), who also mention several metal grains showing alteration to a "rusty" component.

Chemistry

Haskin et al. (1973) determined the major and trace element chemistry of the glass and interior rock fragment (table 1 and figure 6) and note that the glass can not simply be derived from the included rock fragment. Ganapathy et al. (1974) determined the trace and volatile composition and note that the volatile-rich glass may be from South Ray Crater (confirmed by Hertogen et al. 1977). The composition of the glass splashed on the outside of the rock has also been studied by See et al. (1986) and Morris et al. (1986).

The interior rock fragment does not appear to be "pristine" (Ir = 2.25 ppb).

Radiogenic age dating

None

Cosmogenic isotopes and exposure ages

The ^{81}Kr exposure age of 64455 is 2.01 m.y. and the rock is associated with the South Ray cratering event

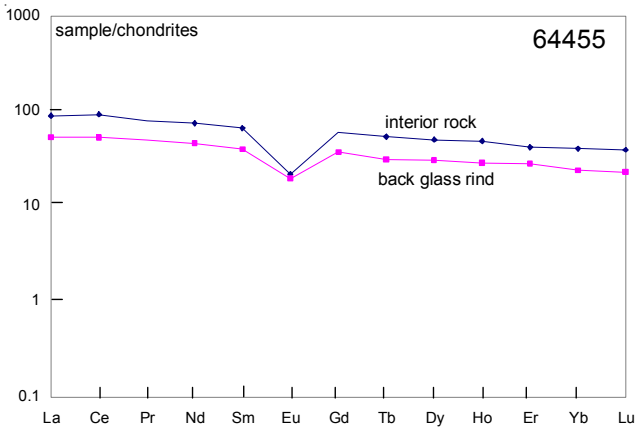

Figure 6: Normalized rare earth element plot for basaltic interior fragment and glass coating of 64455 (data from Haskin et al. 1973).

(Marti 1975, as reported by Arnold et al. 1993). Bogard and Gibson (1975) reported a ^{21}Ne cosmic ray exposure age of 1.2 m.y. and ^{36}Ar age of 1.8 m.y.

Nishiizumi et al. (1995) determined the ^{10}Be, ^{26}Al (figure 7) and ^{36}Cl activity by accelerator mass spectrometry of 19 sub-samples along a depth profile in 64455,82 (slab B). The distribution of microcraters and the ^{10}Be activity are consistent with exposure of 64455 to cosmic rays for only 2 m.y. (Nishiizumi et al. 1995).

Arnold et al. (1993) also determined the ^{10}Be, ^{26}Al and ^{36}Cl as a function of depth below the surface of the protected side of 64455,82, by grinding away (peeling) thin surfaces with a drill.

Other Studies

Neukum et al. (1973) studied the distribution of micrometeorite craters (figure 8). Blanford et al. (1974, 1975) studied the nuclear tracks (figure 9) and present a figure illustrating the lunar orientation (figure 10).

Leich et al. (1973) determined the depth distribution of H and F in exterior chips. Goldberg et al. (1976) attempted to determine solar wind implanted carbon.

Processing

Two slabs have been cut from top to bottom of 64455 (figure 11). Slab A was prepared in 1972 (figure 12). Slab B was cut in 1992 (figure 13). Figure 14 illustrates the saw cuts on the T1 surface.

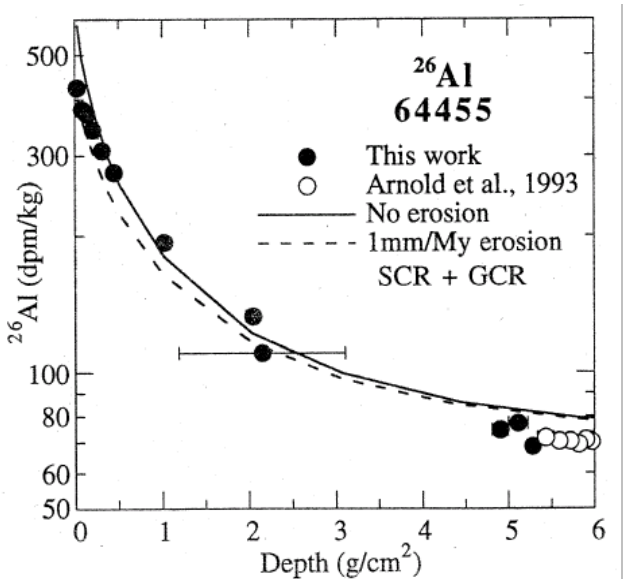

Figure 7: Depth profile for 26Al activity in 64455 (this is figure 2 from Nishiizumi et al. 1995).

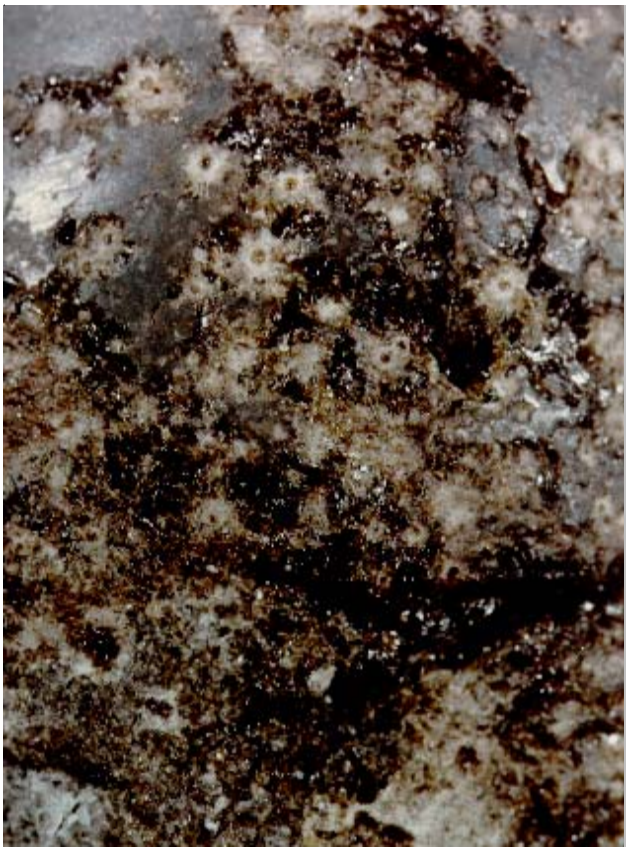

Figure 8: Closeup photo of zap pits illustrating glass-lined pits with surrounding spall zones. Luckly, non of these impacts was large enough to disturb the orientation, although one may have been big enough to break the glass coating, exposing the interior rock sample. The uppermost surface was saturated with small craters (Neukum et al 1973). A few microcraters can also be seen on the exposed rock surface.

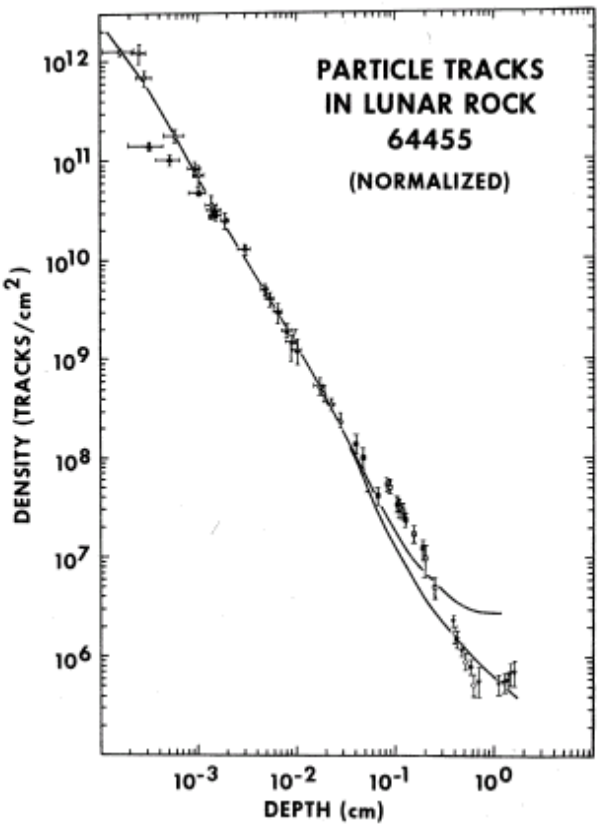

Figure 9: Cosmic ray particle tracks as a function of depth in 64455 (Blanford et al. 1975).

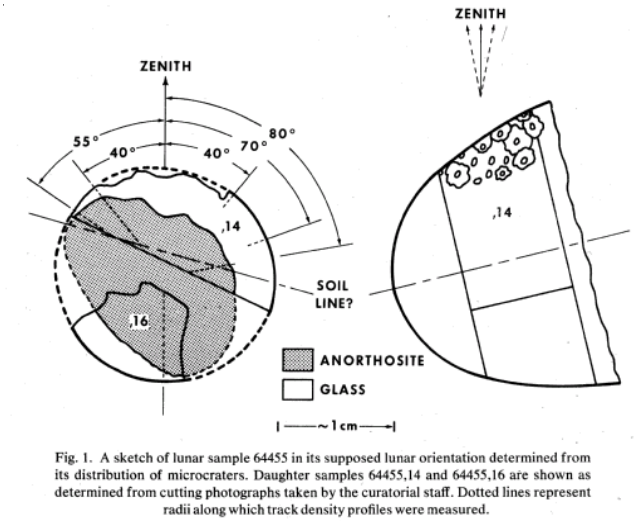

Fig. 1. A sketch of lunar sample 64455 in its supposed lunar orientation determined from its distribution of microcraters. Daughter samples 64455,14 and 64455,16 are shown as determined from cutting photographs taken by the curatorial staff. Dotted lines represent radii along which track density profiles were measured.

Figure 10: Orientation of 64455 from Blanford et al. (1975).

Note: The initial PET photography (with the sample in an upside down orientation, resting on the zap-pitted surface, figure 1) established the orientation cube with the B_1 surface being the zap-pitted surface. This has caused a lot of confusion.

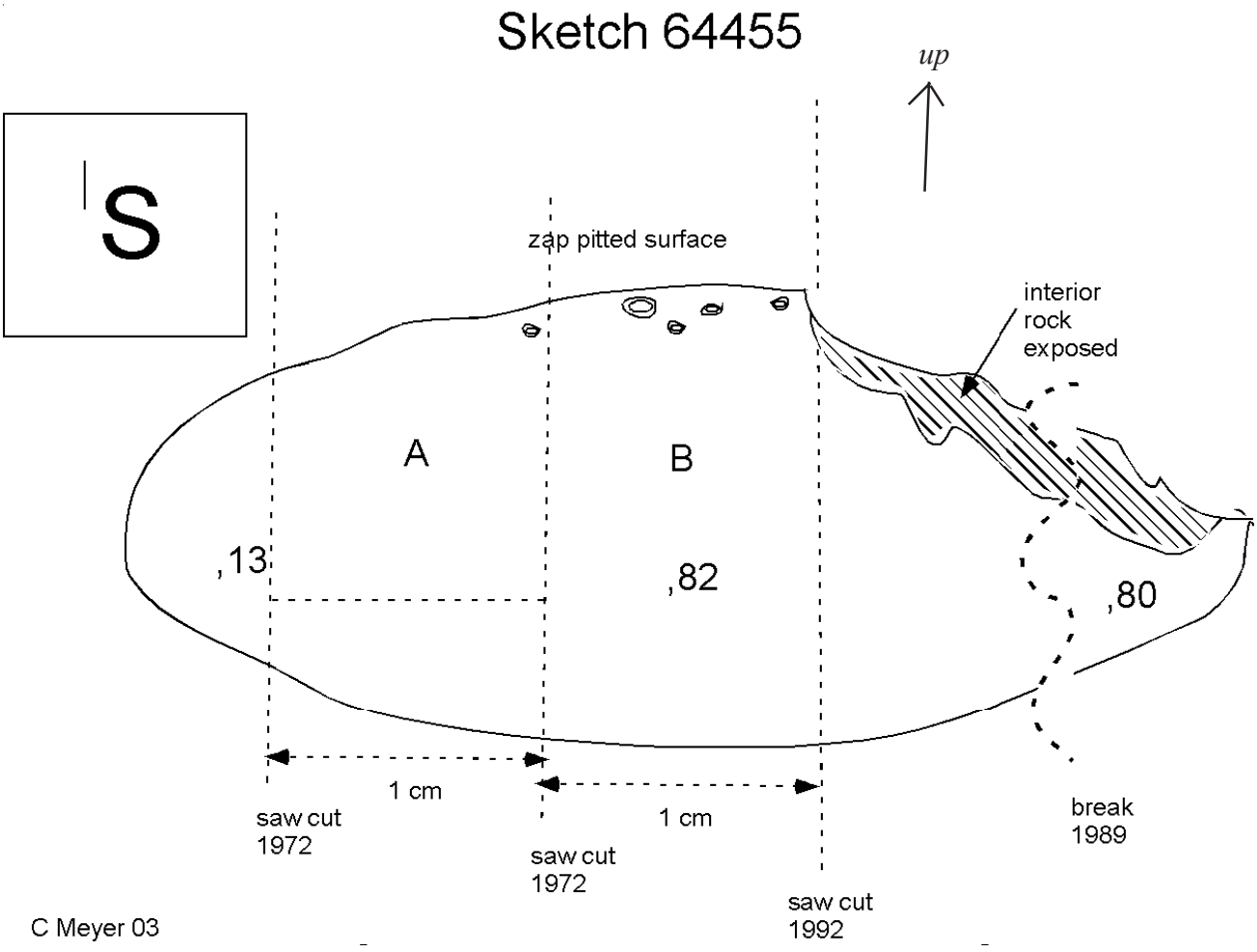

Figure 11: Schematic sketch of glass egg 64455 showing approximate positions of saw cuts to obtain two slabs for accurate depth profile studies of cosmogenic nuclides. Compare with figure 1.

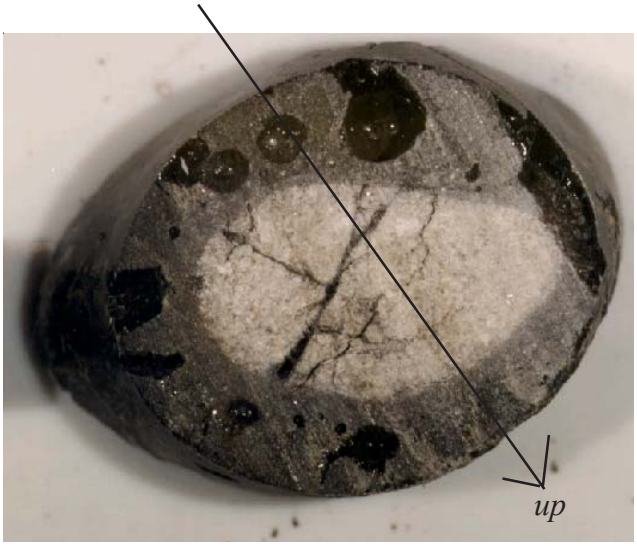

Figure 12: Photo of E1 surface of slab B (64455,82), side next to slab A, showing vesicles in thick black glass and glass veins in rock. NASA # S91-36325

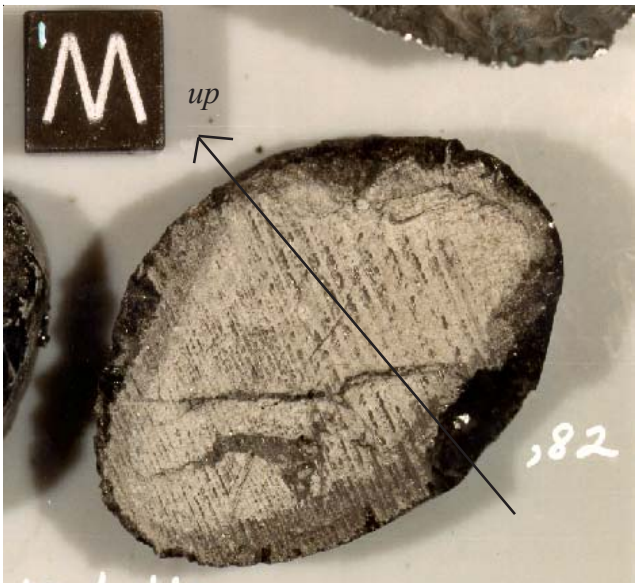

Figure 13: Photo of W1 surface of slab B (64455,82). from NASA # S91-36324 (orientation uncertain)

Table 1. Chemical composition of 64455.

reference	Haskin 73	Haskin 73		Ganapathy 74			Grieve and Plant 73			Morris 86	
weight		glass		rock	glass		rock	glass		glass	
SiO2 %	48.5	44.6	(a)				47.17	45.2	(d)	44.76	(d)
TiO2	0.65	0.45	(a)				0.6	0.39	(d)	0.44	(d)
Al2O3	22.4	25.2	(a)				24.96	24.75	(d)	25.84	(d)
FeO	5.47	6.15	(a)				5.28	6.4	(d)	5.6	(d)
MnO	0.074	0.081	(b)				0.06	0.04	(d)	0.06	(d)
MgO	9.29	7.76	(a)				7.76	8.34	(d)	8.07	(d)
CaO	13.4	14.5	(a)				13.54	14.44	(d)	14.31	(d)
Na2O	0.57	0.37	(b)				0.28	0.44	(d)	0.36	(d)
K2O	0.245	0.106	(a)				0.21	0.05	(d)	0.13	(d)
P2O5											
S %											
sum											
Sc ppm	7.8	7	(b)							6.88	(b)
V											
Cr	1110	1000	(b)							899	(b)
Co	31.1	48.2	(b)							59	(b)
Ni	540	760	(b)	80	905	(c)				927	(b)
Cu											
Zn	4			2.2	2.4	(c)					
Ga	3.05	1.72	(b)								
Ge				62	500	(c)					
As											
Se				190	390	(c)					
Rb	6	3.1	(b)	6.6	3.9	(c)					
Sr											
Y											
Zr											
Nb											
Mo											
Ru											
Rh											
Pd ppb											
Ag ppb				1.2	1.6	(c)					
Cd ppb				5.3	5.2	(c)					
In ppb											
Sn ppb											
Sb ppb				0.45	3.6	(c)					
Te ppb				12.8	38	(c)					
Cs ppm	0.27	0.1	(b)	0.28	0.144	(c)					
Ba										122	(b)
La	21.1	12.6	(b)							12.09	(b)
Ce	56	32.1	(b)							35.1	(b)
Pr											
Nd	34	21	(b)								
Sm	9.8	5.9	(b)							5.88	(b)
Eu	1.23	1.11	(b)							1.14	(b)
Gd		7.4	(b)								
Tb	1.97	1.14	(b)							1.22	(b)
Dy	12.2	7.5	(b)								
Ho	2.7	1.6	(b)								
Er	6.7	4.5	(b)								
Tm											
Yb	6.6	3.92	(b)							3.76	(b)
Lu	0.96	0.56	(b)							0.57	(b)
Hf	7.8	4.3	(b)							4.13	(b)
Ta										0.51	(b)
W ppb											
Re ppb				0.284	4.11	(c)					
Os ppb											
Ir ppb				2.25	40.6	(c)					
Pt ppb											
Au ppb											
Th ppm										2.91	(b)
U ppm				1.43	0.86	(c)				0.54	(b)

technique (a) AA, (b) INAA, (c) RNAA, (d) elec. Probe (broad beam)

Figure 14: Photo of the T1 surface (lunar bottom) of 64455 after cutting first slab A. The approximate location of the second slab is indicated by the line. The scale is in mm and the cube is 1 cm. There are no zap pits on this surface as it was below the soil line. Photo # S72-53870.

NASA Photo #s	
S72-40130-40135	PET dusty
S72-43250-43266	PET B&W
S72-48510-48511	color close-ups
S72-53857	
S72-53870-53872	group photos
S73-22655-22659	
S89-39846-39849	
S91-36321-36325	saw cuts
S93-45928	
S93-45939-45942	

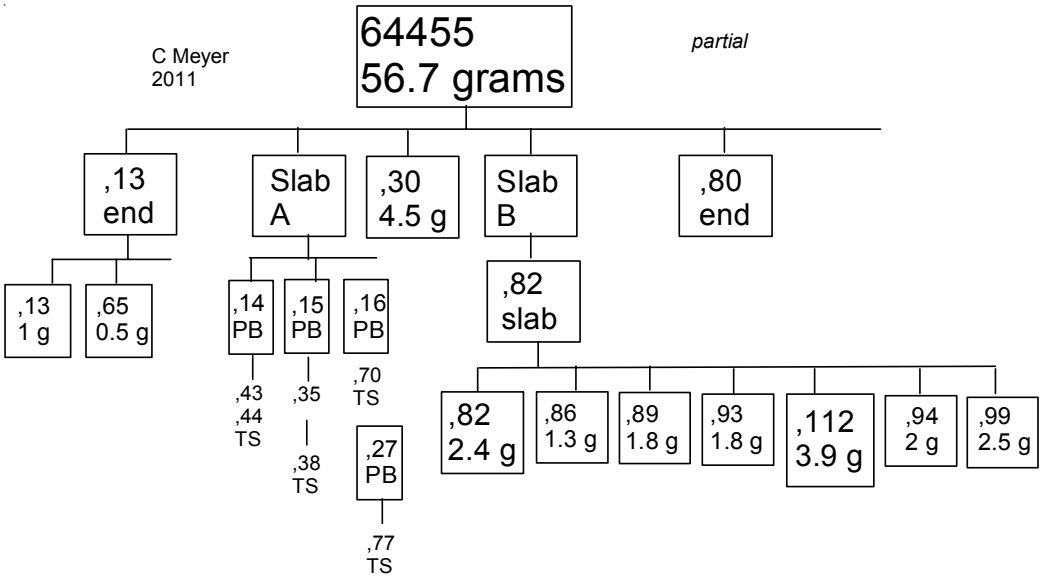

References for 64455

Arnold J.R., Kohl C.P. and Nishiizumi K. (1993) Measurements of cosmogenic nuclides in lunar rock 64455 (abs). *Lunar Planet. Sci.* **XXIV**, 39-40. Lunar Planetary Institute, Houston.

Blanford G.E., Fruland R.M., McKay D.S. and Morrison D.A. (1974a) Lunar surface phenomena: Solar flare track gradients, microcraters, and accretionary particles. *Proc. 5th Lunar Sci. Conf.* 2501-2526.

Bogard D.D., Nyquist L.E., Hirsch W.C. and Moore D.R. (1973b) Trapped solar and cosmogenic noble gas abundances in Apollo 15 and 16 deep drill samples. *Earth Planet. Sci. Lett.* **21**, 52-69.

Bogard D.D. and Gibson E.K. (1975) Volatile gases in breccia 68115 (abs). *Lunar Sci.* **VI**, 63-65. Lunar Planetary Institute, Houston.

Butler P. (1972a) Lunar Sample Information Catalog Apollo 16. Lunar Receiving Laboratory. MSC 03210 Curator's Catalog. pp. 370.

Clark R.S. and Keith J.E. (1973) Determination of natural and cosmic ray induced radionuclides in Apollo 16 lunar samples. *Proc. 4th Lunar Sci. Conf.* 2105-2113.

Ganapathy R., Morgan J.W., Higuchi H., Anders E. and Anderson A.T. (1974) Meteoritic and volatile elements in Apollo 16 rocks and in separated phases from 14306. *Proc. 5th Lunar Sci. Conf.* 1659-1683.

Goldberg R.H., Trombrello T.A. and Burnett D.S. (1976a) Flourine as a constituent in lunar magmatic gases. *Proc. 7th Lunar Sci. Conf.* 1597-1613.

Goldberg R.H., Weller R.A., Trombrello T.A. and Burnett D.S. (1976b) Surface concentrations of F, H and C (abs). *Lunar Sci.* **VII**, 307-309. Lunar Planetary Institute, Houston.

Grieve R.A.F. and Plant A.G. (1973) Partial melting on the lunar surface, as observed in glass coated Apollo 16 samples. *Proc. 4th Lunar Sci. Conf.* 667-679.

Haskin L.A., Helmke P.A., Blanchard D.P., Jacobs J.W. and Telunder K. (1973) Major and trace element abundances in samples from the lunar highlands. *Proc. 4th Lunar Sci. Conf.* 1275-1296.

Heiken G.H., Vaniman D.T. and French B. (1991) **Lunar Sourcebook.** Cambridge Univ. Press

Hertogen J., Janssens M.-J., Takahashi H., Palme H. and Anders E. (1977) Lunar basins and craters: Evidence for systematic compositional changes of bombarding population. *Proc. 8th Lunar Sci. Conf.* 17-45.

Hunter R.H. and Taylor L.A. (1981) Rust and schreibersite in Apollo 16 highland rocks: Manifestations of volatile-element mobility. *Proc. 12th Lunar Planet. Sci. Conf.* 253-259.

Leich D.A., Tombrello T.A. and Burnett D.S. (1973a) The depth distribution of hydrogen and fluorine in lunar samples. *Earth Planet. Sci. Lett.* **19**, 305-314.

Leich D.A., Tombrello T.A. and Burnett D.S. (1973b) The depth distribution of hydrogen and fluorine in lunar samples. *Proc. 4th Lunar Sci. Conf.* 1597-1612.

Leich D.A., Goldberg R.H., Burnett D.S. and Tombrello T.A. (1974) Hydrogen and fluorine in the surfaces of lunar samples. *Proc. 5th Lunar Sci. Conf.* 1869-1884.

LSPET (1973b) The Apollo 16 lunar samples: Petrographic and chemical description. *Science* **179**, 23-34.

LSPET (1972c) Preliminary examination of lunar samples. *In* Apollo 16 Preliminary Science Report. NASA SP-315, 7-1—7-58.

Morris R.V., See T.H. and Horz F. (1986) Composition of the Cayley Formation at Apollo 16 as inferred from impact melt splashes. *Proc. 17th Lunar Planet. Sci. Conf.* in J. Geophys. Res. **90**, E21-E42.

Moore C.B. and Lewis C.F. (1976) Total nitrogen contents of Apollo 15, 16 and 17 lunar rocks and breccias (abs). *Lunar Sci.* VII, 571-573. Lunar Planetary Institute, Houston.

Neukum G., Horz F., Morrison D.A. and Hartung J.B. (1973) Crater populations on lunar rocks. *Proc. 4th Lunar Sci. Conf.* 3255-3276.

Nishiizumi K., Kohl C.P., Arnold J.R., Finkel R.C., Chaffee M.W., Masarik J. and Reedy R.C. (1995) Final results of comogenic nuclides in lunar rock 64455 (abs). *Lunar Planet. Sci.* **XXVI,** 1055-1056. Lunar Planetary Institute, Houston.

Ryder G. and Norman M.D. (1980) Catalog of Apollo 16 rocks (3 vol.). Curator's Office pub. #52, JSC #16904

Schaal R.B., Hörz F., Thompson T.D. and Bauer J.F. (1979a) Shock metamorphism of granulated lunar basalt. P*roc. 10th Lunar Planet. Sci. Conf.* 2547-2571.

See T.H., Horz F. and Morris R.V. (1986) Apollo 16 impact-melt splashes: Petrography and major-element composition. *Proc. 17th Lunar Planet. Sci. Conf.* in J. Geophys. Res. **91**, E3-E20.

Sutton R.L. (1981) Documentation of Apollo 16 samples. In Geology of the Apollo 16 area, central lunar highlands. (Ulrich et al.) U.S.G.S. Prof. Paper 1048.

Ulrich D.R. and Weber J. (1973) Correlation of the thermal history of lunar and synthetic glass by DTA and X-ray techniques. *In Lunar Science* **IV**, 743-744. Lunar Science Institute, Houston.

Vaniman D.T. and Papike J.J. (1980) Lunar highland melt rocks: Chemistry, petrology and silicate mineralogy. *In* Proc. **Conf. Lunar Highlands Crust** (Papike J.J. and Merrill R.B., eds.) 271-337. Pergamon. Lunar Planetary Institute, Houston.